A molecularly defined neural circuit for cold defense revealed by targeted single-nucleus transcriptomic mapping

Supplementary materials

Contents:

Extended Data Fig. 1

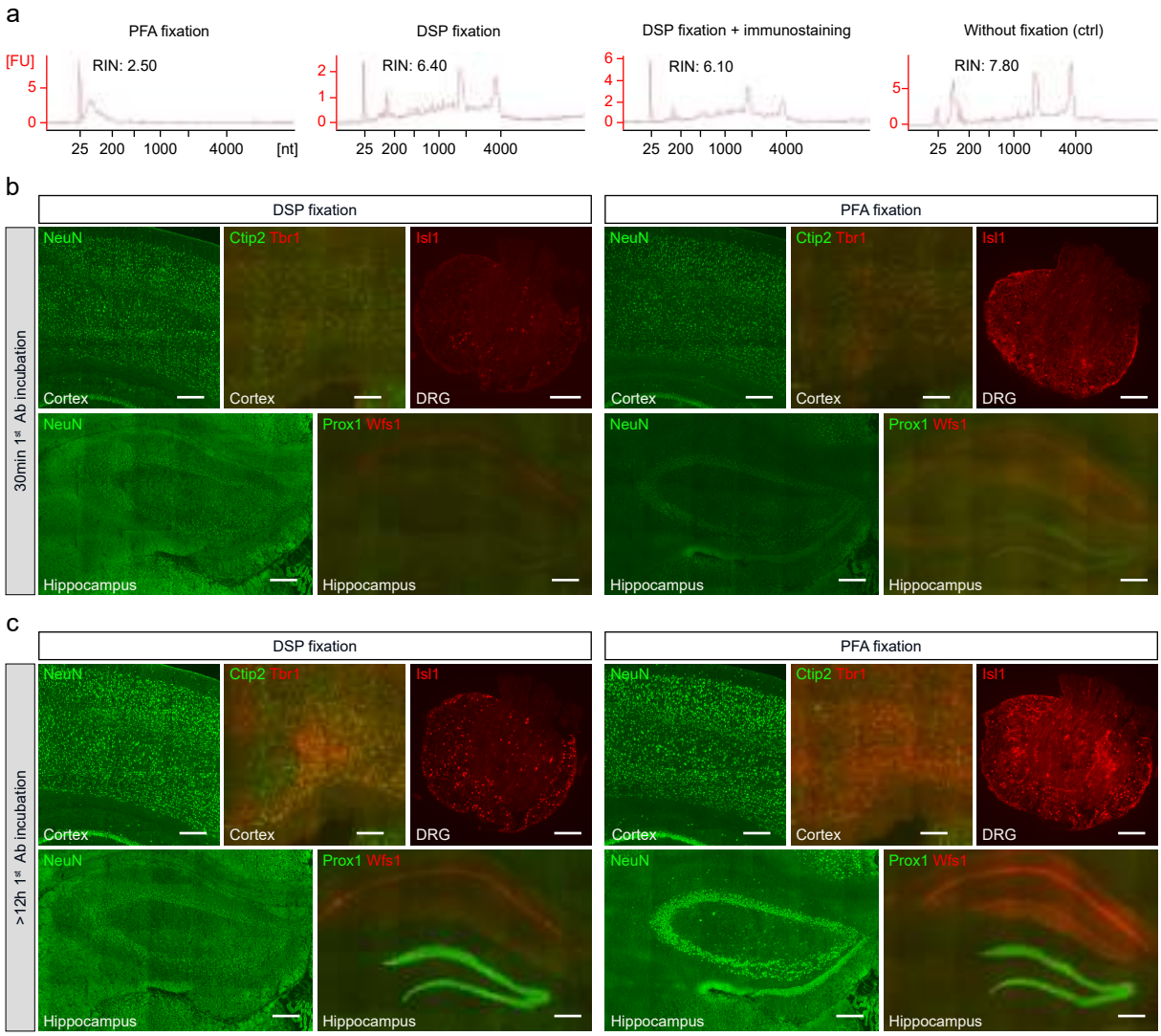

Extended Data Fig. 1 Assessment of the modified immunostaining method.

a, RNA integrity (RIN) assessment of total RNA samples extracted from consecutive sections of the same mouse brain fixed with PFA or DSP for comparison. DSP-fixed samples were incubated with DTT; one of the two DSP-fixed samples was stained with the FOS antibody using the optimized protocol before RNA extraction. A sample of fresh-frozen sections was taken as a positive control in RNA integrity analysis. A higher RIN value indicates better RNA integrity. **b**-**c**, Detection of various neuronal markers (NeuN, Ctip2, Tbr1, Isl1, Prox1, and Wfs1) expressing in the peripheral and central nervous systems on the sections fixed by DSP (left panels in **b**,**c**) or PFA (right panels in **b**,**c**), with short (30 min; **b**) or long (>12 h; **c**) primary antibody incubations. Scale bars in **b,c**: 100 µm.

Extended Data Fig. 2

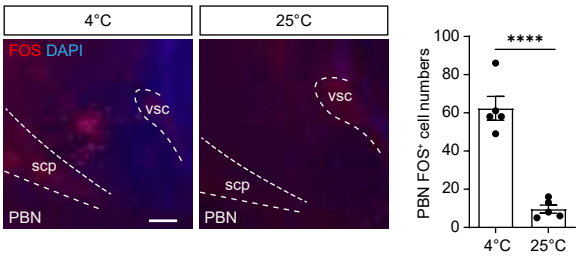

Extended Data Fig. 2 Cold-activated neurons in the PBN recognized by FOS immunostaining.

FOS immunostaining in the PBN of wild-type mice exposed to 4°C vs. 25°C. FOS^+ cell numbers were compared between 4°C and 25°C (n=5 mice per group). Statistical analysis used two-tailed unpaired Student's *t*-test. Scale bar: 200 µm.

Extended Data Fig. 3

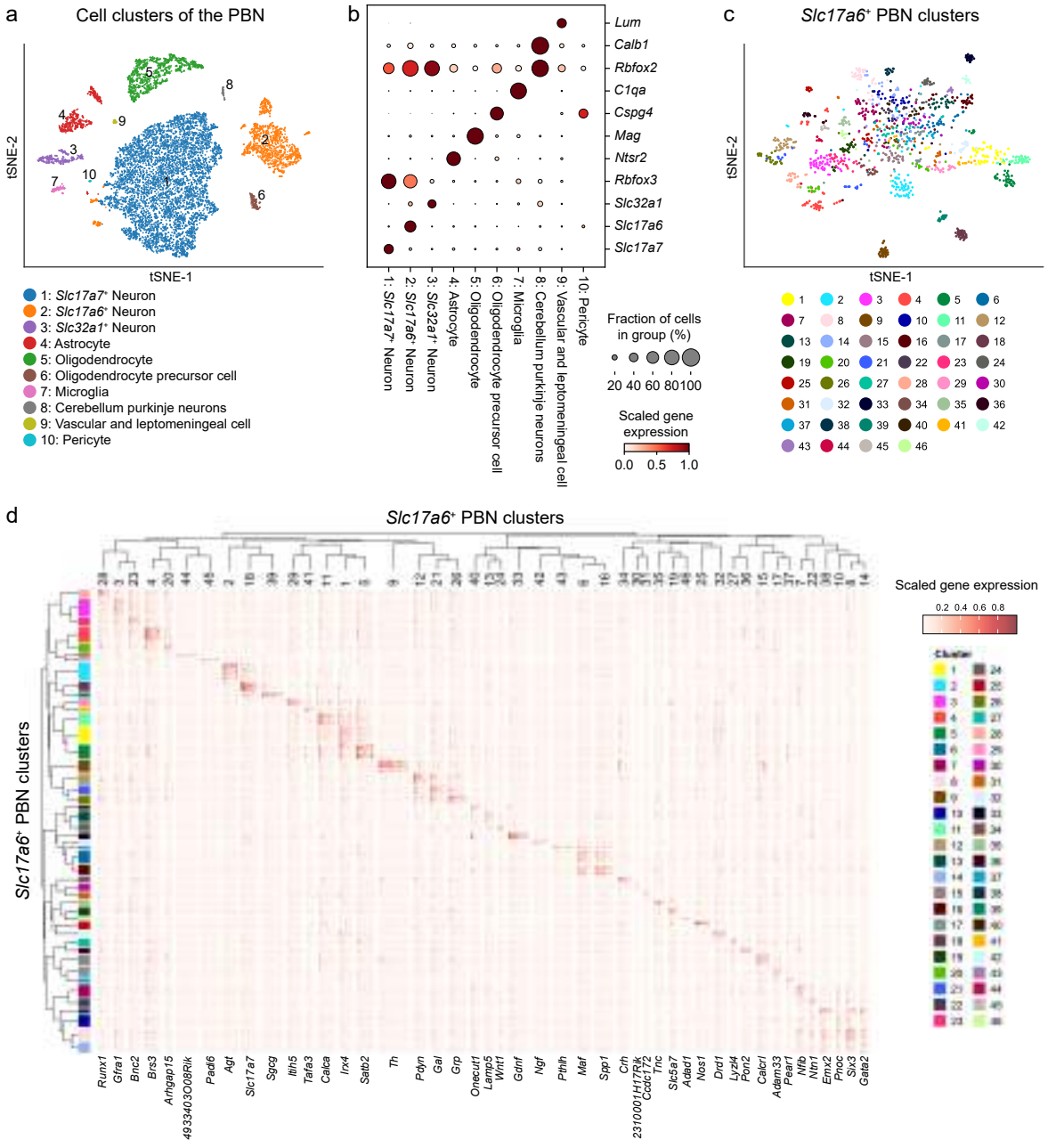

Extended Data Fig. 3 Generation of a new PBN cell atlas using high-throughput snRNA-seq. **a**, tSNE plot of cell populations in the PBN of wild-type mice. **b**, Bubble plot of marker genes defining major PBN cell types. **c**, tSNE plot of *Slc17a6*$^{+}$ neuronal clusters of the PBN and its adjacent areas. **d**, Heatmap of cluster-specific marker genes of *Slc17a6*$^{+}$ neurons (see Supplementary Table 1 for the marker gene list). **e**, Bubble plot of canonical markers for the PBN neurons studied previously.

Extended Data Fig. 4

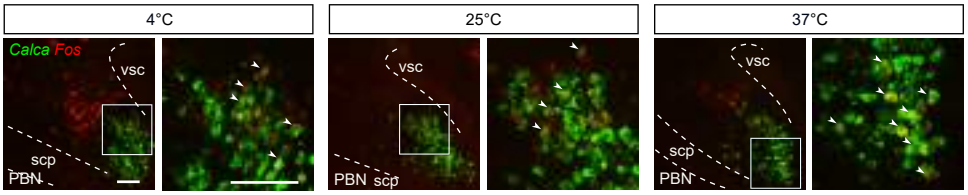

Extended Data Fig. 4 Co-expression of *Fos* and *Calca* in the PBN of the mice at different ambient temperatures.

smFISH showing *Fos* and *Calca* co-expression in the elPBN of mice exposed to 4°C, 25°C, and 37°C. Arrowheads indicate the neurons co-expressing *Calca* and *Fos*. Scale bar: 100 µm.

Extended Data Fig. 5

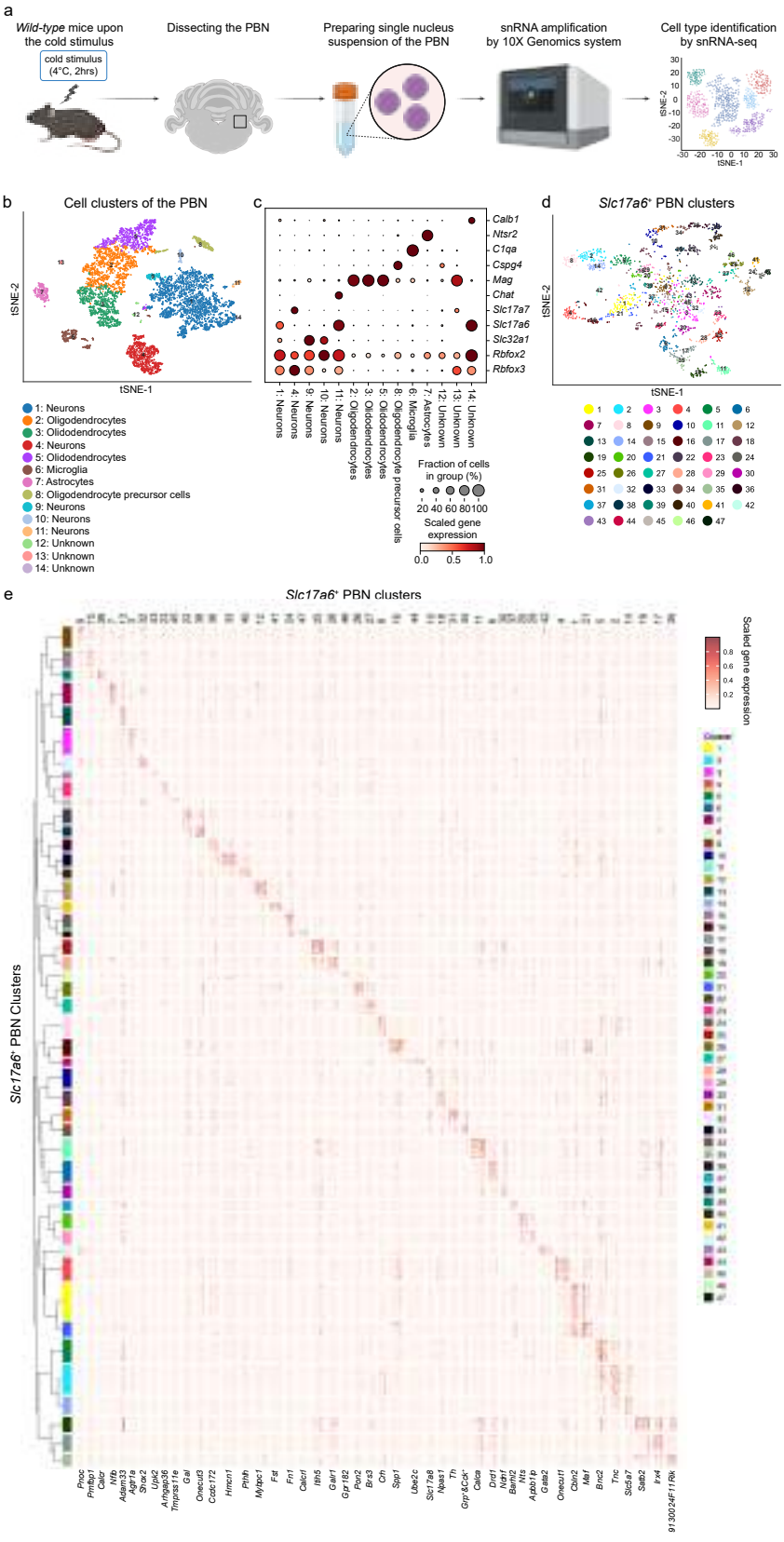

Extended Data Fig. 5 A new PBN cell atlas of cold-treated mice obtained by high-throughput single-nucleus RNA-seq.

a, Schematic workflow of the single-nucleus RNA-seq experiment to establish a new PBN cell atlas from cold-treated wild-type mice using 10x Genomics platform. **b**, tSNE plot of nuclei isolated from the PBN and adjacent areas in cold-treated mice. **c**, Bubble plot of marker gene expression defining major PBNs cell types. **d**, tSNE plot of *Slc17a6*$^{+}$ neuronal clusters in the PBN and adjacent areas. **e**, Heatmap of marker genes for each subtype of *Slc17a6*$^{+}$ neurons (see Supplementary Table 2 for marker gene list).

Extended Data Fig. 6

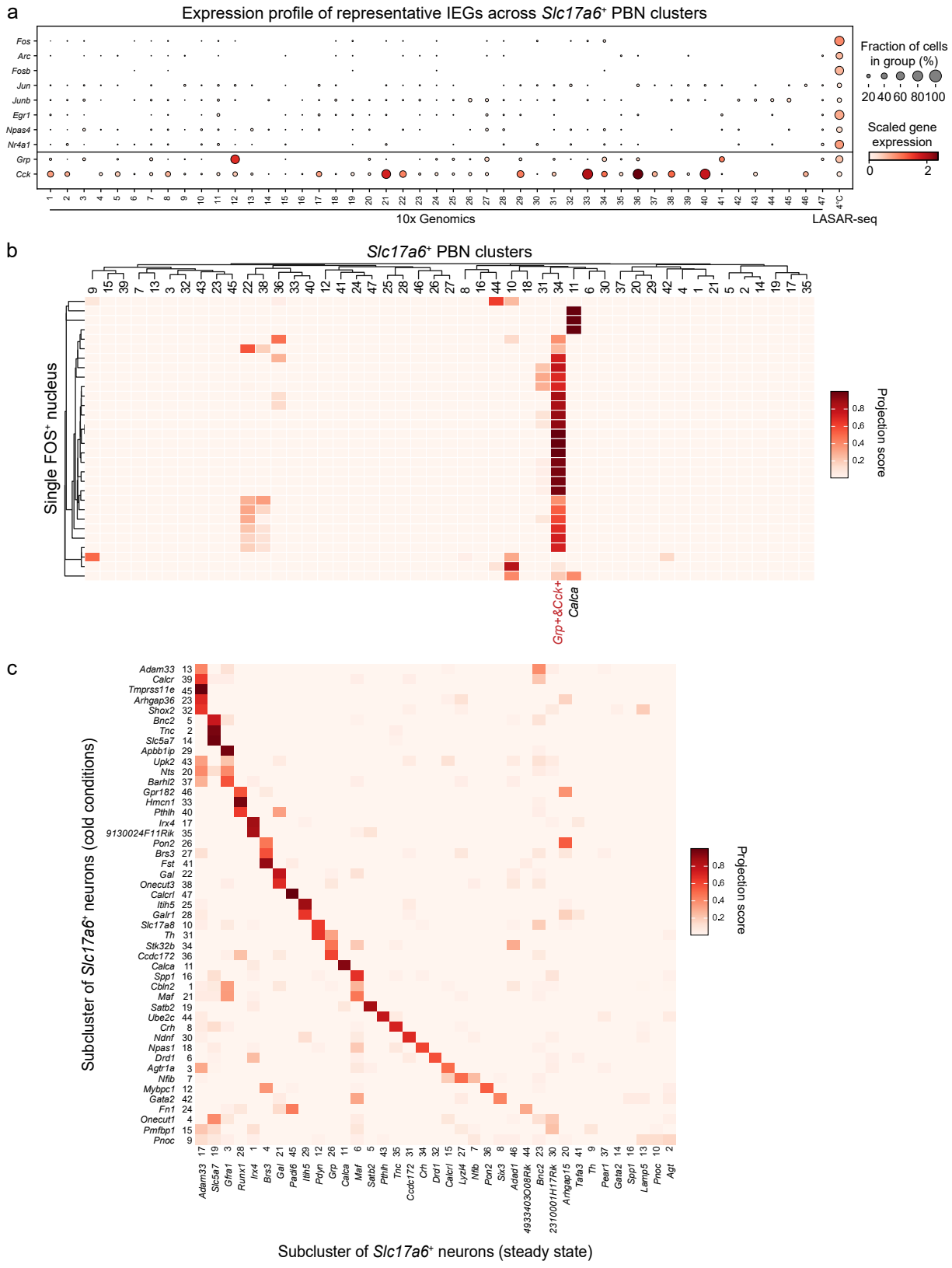

Extended Data Fig. 6 Comparison of cold-activation parabrachial neurons analyzed by high-throughput snRNA-seq or LASAR-seq.

a, Bubble plots showing the expression of immediate-early genes across *Slc17a6*$^{+}$ PBN clusters from cold-treated mice, compared to the cold-induced FOS^{+} neurons identified by LASAR-seq (last column on the right). **b**, Heatmap of mapping the cold-activated neurons analyzed by LASAR-seq to the new PBN atlas from cold-treated mice as reference. **c**, Heatmap showing the transcriptomic similarity between PBN cell atlases from the mice at steady state and stimulated by 4°C cold.

Extended Data Fig. 7

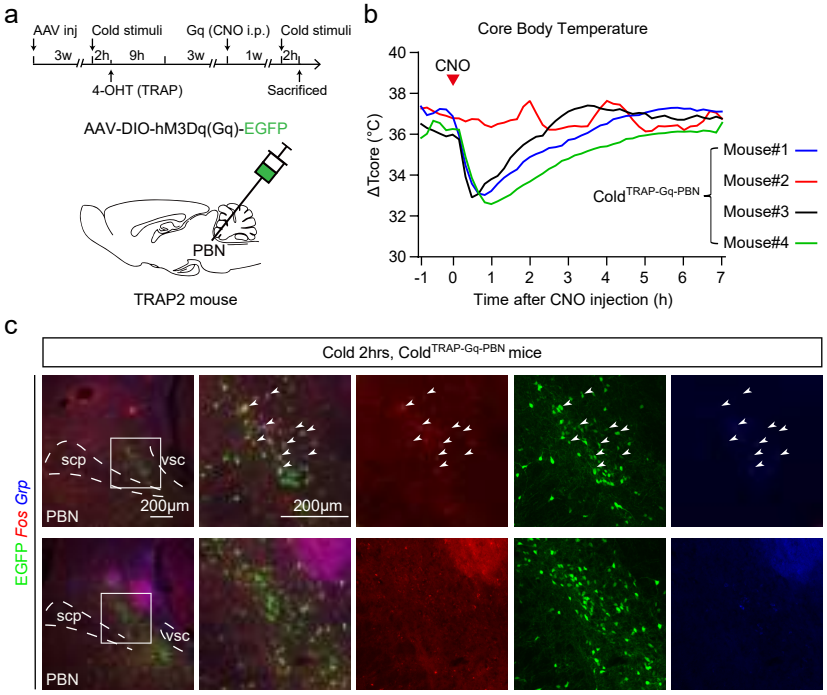

Extended Data Fig. 7 Analyzing cold-activated PBN neurons using the FosTRAP2 method.

a, Schematic illustration of the TRAP2 experiment to label and re-activate cold-activated neurons using AAV vectors encoding DIO-hM3Dq(Gq)-EGFP. For cross-validation with the endogenous FOS expression induced by a cold stimulus, the mice were exposed to 4°C for 2h before sacrifice. **b**, Chemogenetic re-activation of the TRAP2-labeled neurons and T_{core} telemetry recording. **c**, Fluorescent images of combinatorial immunostaining of EGFP ("cold-trapped" cell marker) and smFISH of *Fos* and *Grp* for analyzing their colocalization. Enlarged images of the rectangular areas were shown next to the first column. White arrowheads point to the cells co-expressing EGFP, *Fos*, and *Grp*. Scale bar: 200μm.

Extended Data Fig. 8

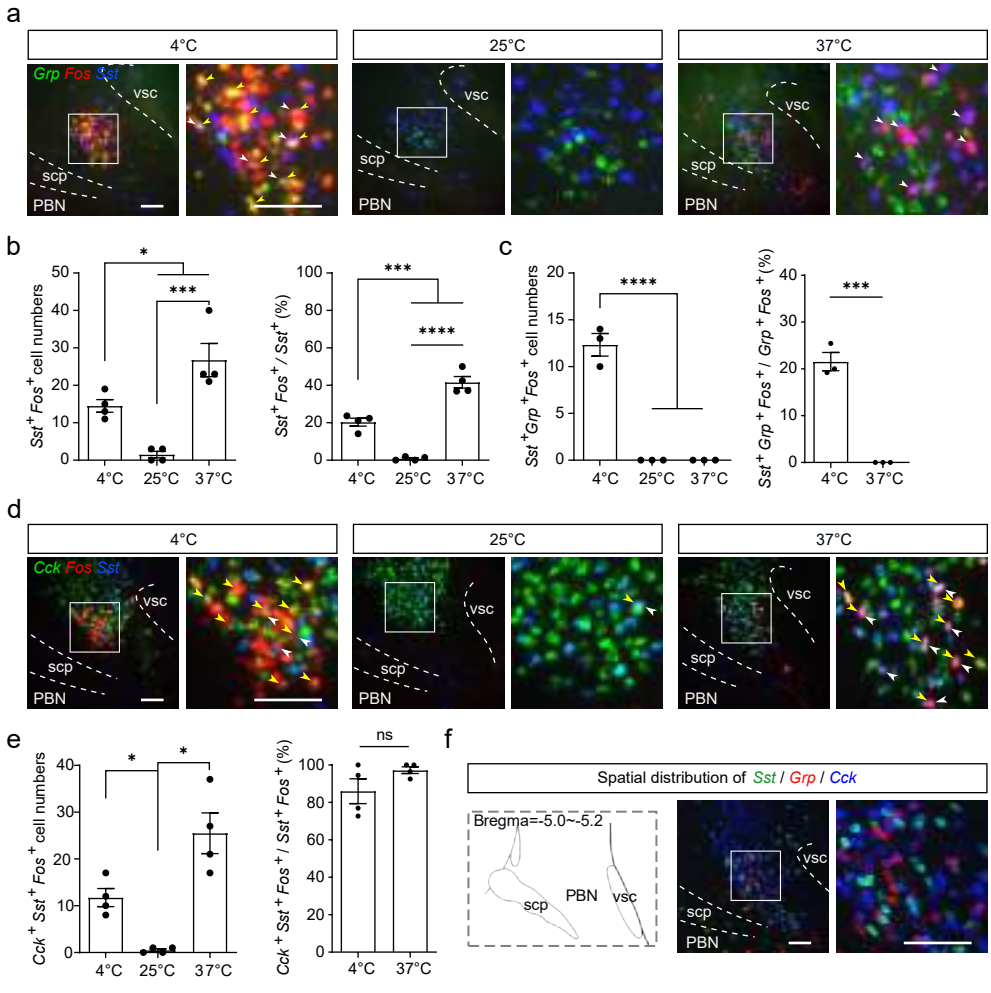

Extended Data Fig. 8 *Sst*$^+$ PBN neurons respond to both cold and warm stimuli.

a, smFISH images showed *Fos, Sst*, and *Grp* expression in the PBN of mice exposed to 4°C, 25°C, or 37°C. White arrowheads point to the neurons co-expressing *Sst* and *Fos*, and the yellow ones point to the neurons co-expressing *Grp* and *Fos*. **b**, Numbers of *Sst* and *Fos* co-expressing neurons at 4°C, 25°C, or 37°C; percentages of *Fos*$^+$ activated neurons among *Sst*$^+$ cells (*Fos*$^+$ *Sst*$^+$ / *Fos*$^+$) at 4°C, 25°C, or 37°C (n=4 mice per group). **c**, Numbers of *Sst*, *Grp*, and *Fos* triple co-expressing neurons at 4°C, 25°C, or 37°C; percentages of *Sst*$^+$ neurons among the activated *Grp*$^+$ cells (*Sst*$^+$ *Grp*$^+$ *Fos*$^+$ / *Grp*$^+$ *Fos*$^+$) at 4°C or 37°C (n=3 mice per group). **d**, smFISH images showed *Fos, Sst*, and *Cck* in the PBN of mice exposed to 4°C, 25°C, or 37°C. White arrowheads point to the neurons co-expressing *Sst* and *Fos*, and the yellow ones point to the neurons co-expressing *Cck* and *Fos*. **e**, Numbers of *Cck*, *Sst*, and *Fos* triple co-expressing neurons at 4°C, 25°C, or 37°C; percentages of *Cck*$^+$ neurons among the activated *Sst*$^+$ cells (*Cck*$^+$ *Sst*$^+$ *Fos*$^+$ / *Sst*$^+$ *Fos*$^+$) at 4°C or 37°C (n=4 mice per group). **f**, Spatial distribution of *Sst*$^+$, *Grp*$^+$, or *Cck*$^+$ neurons in the PBN examined by smFISH. Statistical analyses used one-way ANOVA followed by Bonferroni's test in **b**, **c**, and **e**. Scale bars in **a,d,** and **f**: 50 μm.

Extended Data Fig. 9

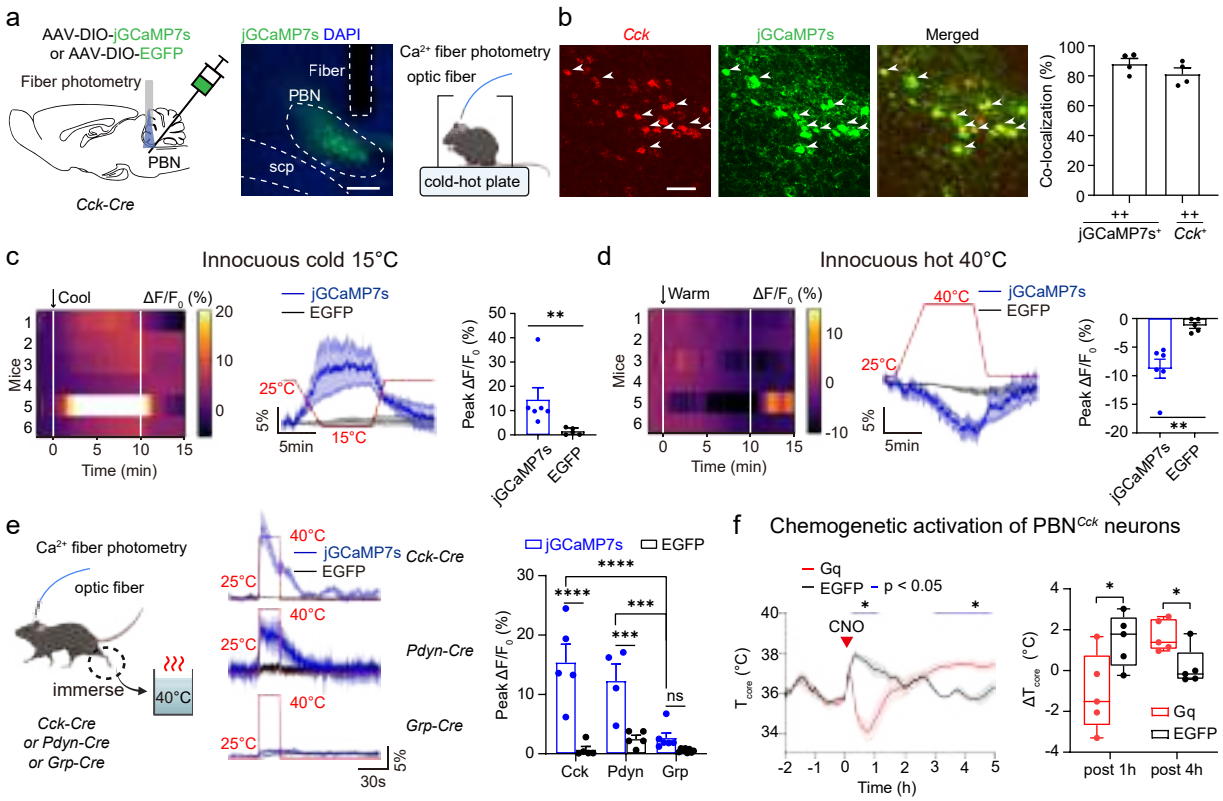

Extended Data Fig. 9 *Cck*$^{+}$ PBN neurons respond to both cold and warm stimuli.

a, Scheme of Ca^{2+} fiber photometry experiment in *Cck-Cre* mice stimulated by different temperatures using a cold-hot plate. jGCaMP7s or EGFP was introduced in *Cck*^{PBN} neurons via AAV injection. **b**, Representative images and quantitative analysis showing jGCaMP7s expression in *Cck*^{PBN} neurons. Arrowheads point to the neurons co-expressing jGCaMP7s and *Cck*. The bar plot shows co-expression ratios among jGCaMP7s^{+} or *Cck*$^{+}$ neurons (n=4 mice). **c**-**d**, Heatmap of Ca^{2+} signals, averaged Ca^{2+} traces, and bar plot of peak $\Delta F/F_0$ for *Cck*^{PBN} neurons during 15°C (**c**) or 40°C (**d**) innocuous stimuli (jGCaMP7s: n=6 mice; EGFP: n=5 mice). The stimulating duration is indicated between two vertical white lines in the heatmaps. **e**, Scheme and results of Ca^{2+} fiber photometry experiment upon another paradigm of warm stimuli induced by immersing one hind limb of *Cck-Cre, Pdyn-Cre,* or *Grp-Cre* mice expressing jGCaMP7s or EGFP (control) into 40°C water for 20 s. Averaged Ca^{2+} traces and peak $\Delta F/F_0$ for jGCaMP7s-expressing *Cck*$^{+}$, *Pdyn*$^{+}$, or *Grp*$^{+}$ PBN neurons and EGFP controls were compared upon 40°C warm stimulus (n=5, 4, 6 for jGCaMP7s group; n=5, 5, 8 for EGFP group in *Cck-Cre*, *Pdyn-Cre*, and *Grp-Cre* mice). **f**, T_{core} traces of *Cck-Cre* mice expressing Gq or EGFP in the PBN upon chemogenetic activation by CNO injection at t=0 hr. ΔT_{core} at t=1 hr and t=4 hr were quantified and shown in the box plot (n=5 mice per group). Statistical significance was analyzed using two-tailed Mann-Whitney test in **c**-**e**, and two-tailed unpaired Student's *t*-test in **f**. Scale bars in **a**: 200 μm; in **b**: 50 μm.

Extended Data Fig. 10

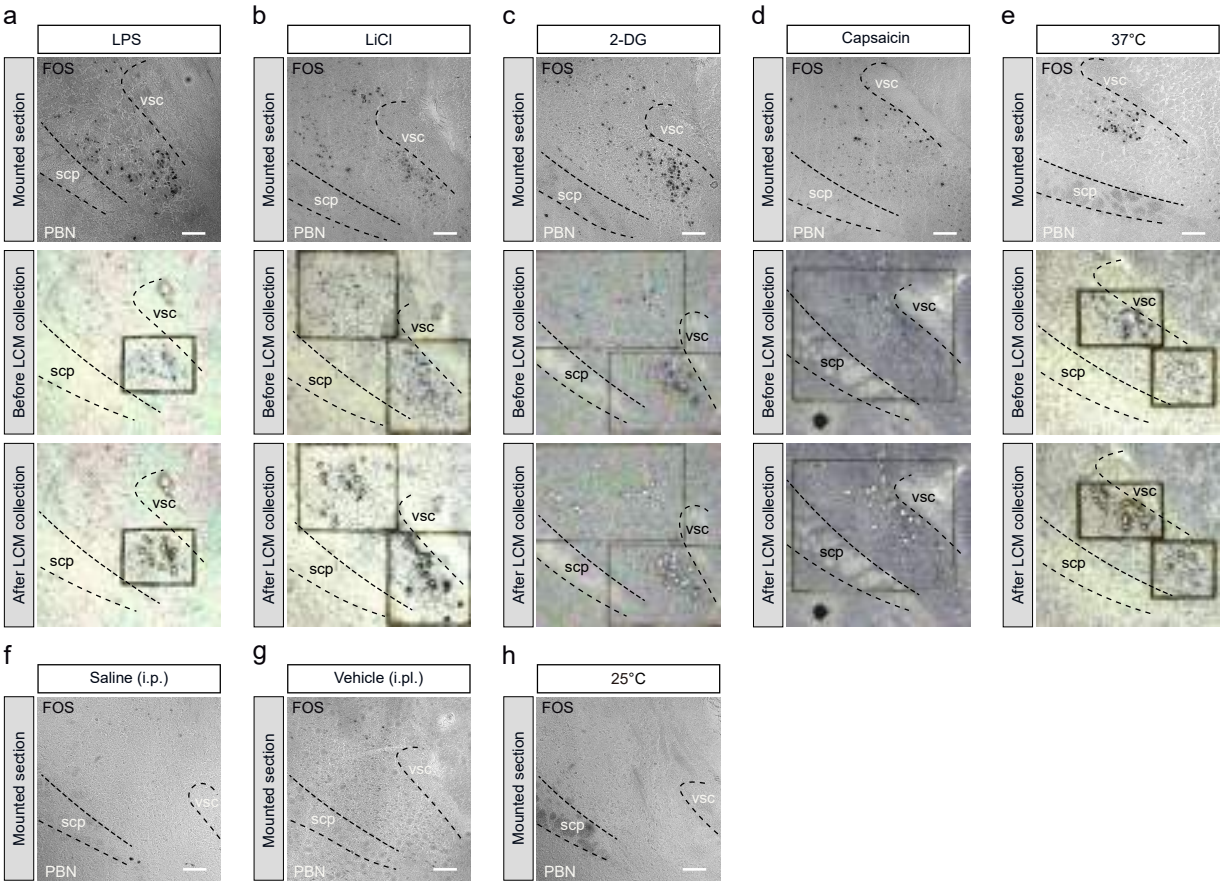

Extended Data Fig. 10 FOS immunostaining and laser microdissection of individual activated neurons in the PBN upon different stimuli.

a-**h** DAB chromogenic FOS immunostaining of PBN in wild-type mice after different stimuli: LPS i.p. (**a**), LiCl i.p. (**b**), 2-DG i.p. (**c**), capsaicin i.pl. (**d**), 37°C warm exposure (**e**) or controls: saline i.p. injection (**f**), 20% ethanol vehicle i.pl. injection (**g**), 25°C exposure (**h**). Images show brain sections on standard slides (1st and 4th rows), and on PEN membrane slides before (2nd row) and after (3rd row) microdissection of the FOS^+ nuclei. Scale bars: 100 µm.

Extended Data Fig. 11

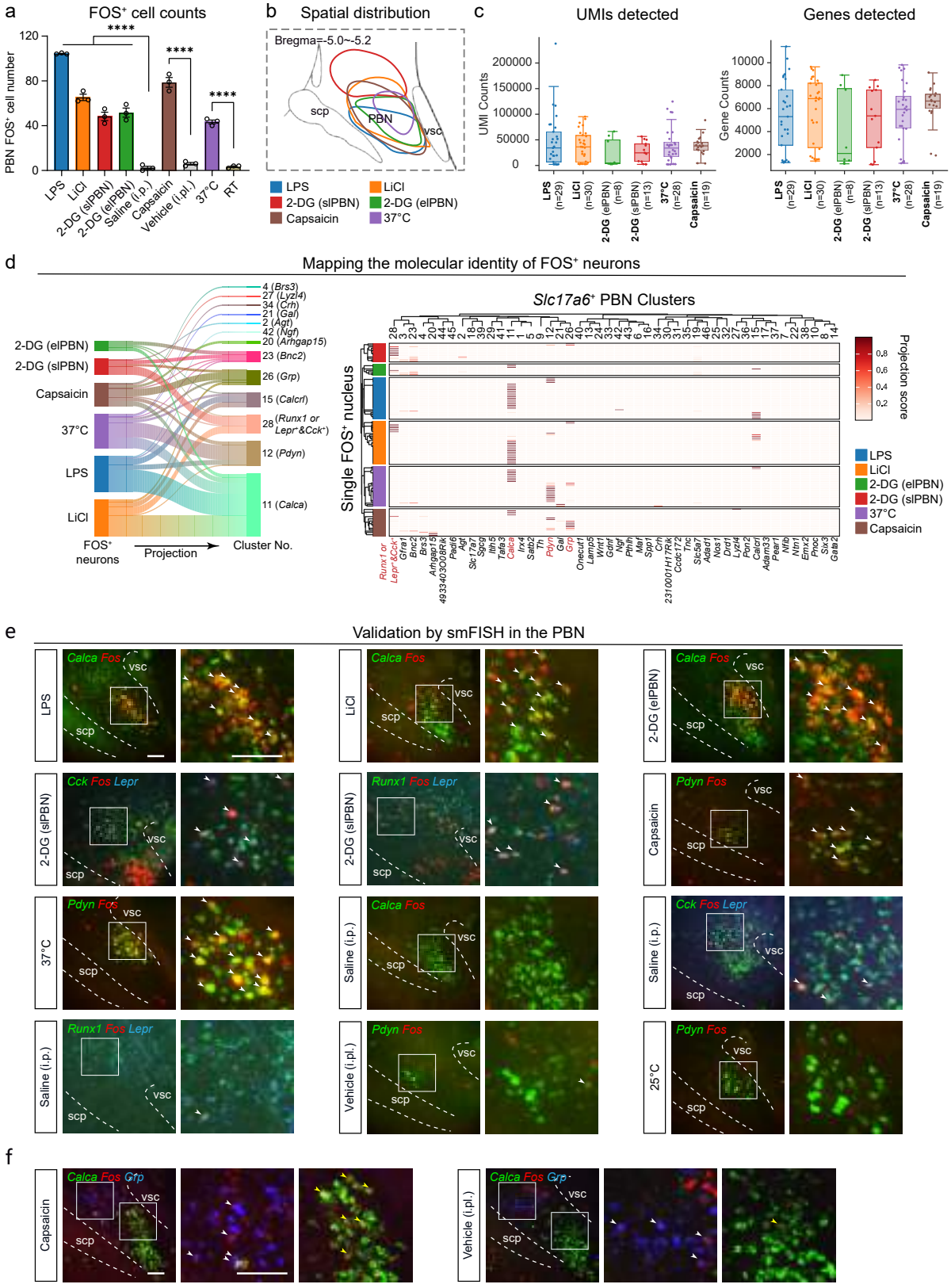

Extended Data Fig. 11 Methodological assessment for LASAR-seq.

a, FOS^+ cell numbers in the PBN across different stimuli (RT: 25°C; n=3 mice per stimulus). **b**, Diagrammatic spatial distribution of sparse FOS^+ neurons in the PBN in response to different stimuli (Bregma: –5.0 to –5.2), with scp (superior cerebellar peduncle) and vsc (ventral spinocerebellar tract) as the anatomical landmarks. **c**, UMI and gene counts of individual FOS^+ neurons; cell numbers passing the quality check are shown in the brackets. **d**, Label transfer analysis of LASAR-seq identifying activated neuronal types with specific molecular markers (Sankey plot, left; heatmap, right); representative marker genes are shown in the brackets of the Sankey plot or at the bottom of the heatmap. The projection scores reflect the correlation between the mapped clusters and the query cells. Marker genes of the activated populations are marked in red in the heatmap. **e-f**, smFISH validation of *Fos* and marker gene co-expression in the PBN after stimuli vs. controls; arrowheads point to the neurons showing co-expression of *Fos* and the corresponding markers. Statistical analysis was performed using one-way ANOVA followed by Bonferroni's test in **b**. Scale bars in **e** and **f**: 100 μm.

Extended Data Fig. 12

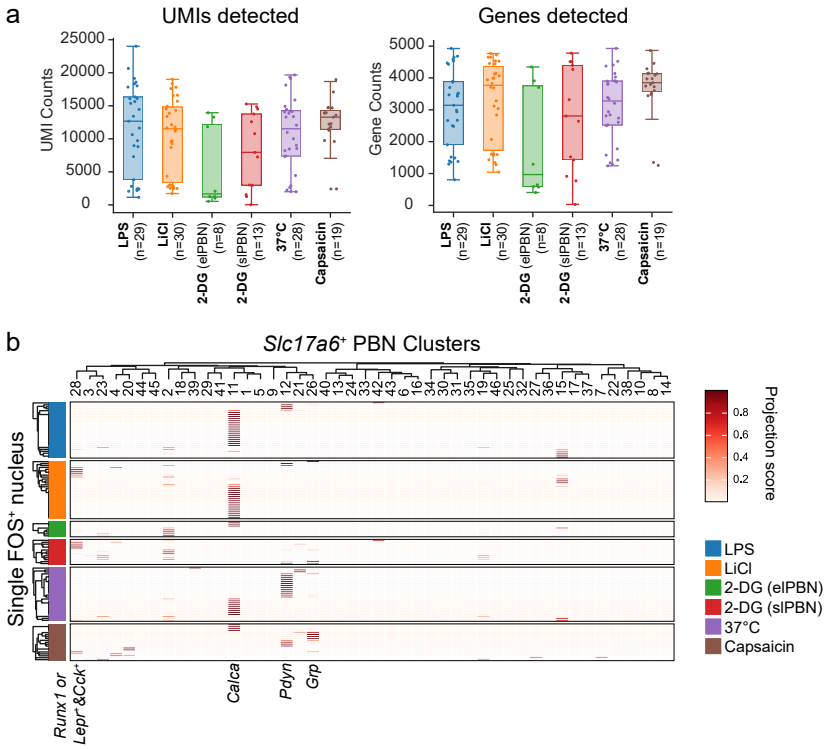

Extended Data Fig. 12 Downsampling the LASAR-seq data recapitulates the cell-type mapping results.

a, UMI and gene counts of the microdissected FOS$^+$ neurons in the PBN upon different stimuli after downsampling the LASAR-seq data to match the high-throughput snRNA-seq depth of parabrachial neurons using 10x Genomics platform; cell numbers passing the quality check are shown in the brackets. **b**, Heatmap showed cell-type identification of sparsely activated neurons based on the downsampled LASAR-seq data with representative marker genes of the selective clusters labeled at the bottom.

Extended Data Fig. 13

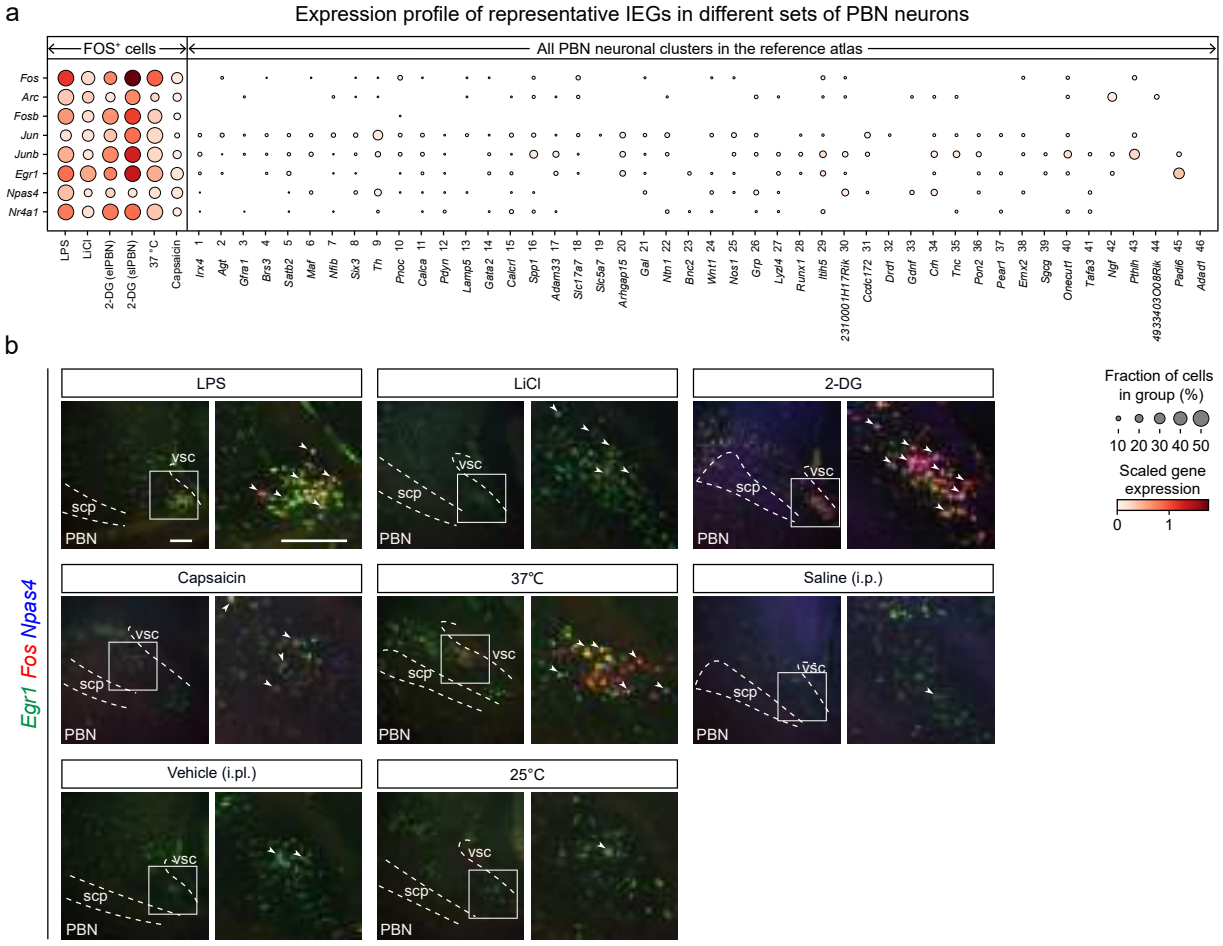

Extended Data Fig. 13 Expression of distinct IEGs in activated PBN neurons.

a, Bubble plot of immediate-early gene expression in distinct sets of activated neurons studied by LASAR-seq experiment and by high-throughput snRNA-seq of all PBN neurons (reference atlas, unstimulated). Stimuli or marker genes are listed at the bottom. **b**, smFISH showed co-expression of *Fos*, *Egr1*, and *Npas4* in the PBN across different stimulation conditions. Arrowheads point to the neurons co-expressing *Fos* and corresponding markers. Scale bars in **b**: 100 µm.

Extended Data Fig. 14

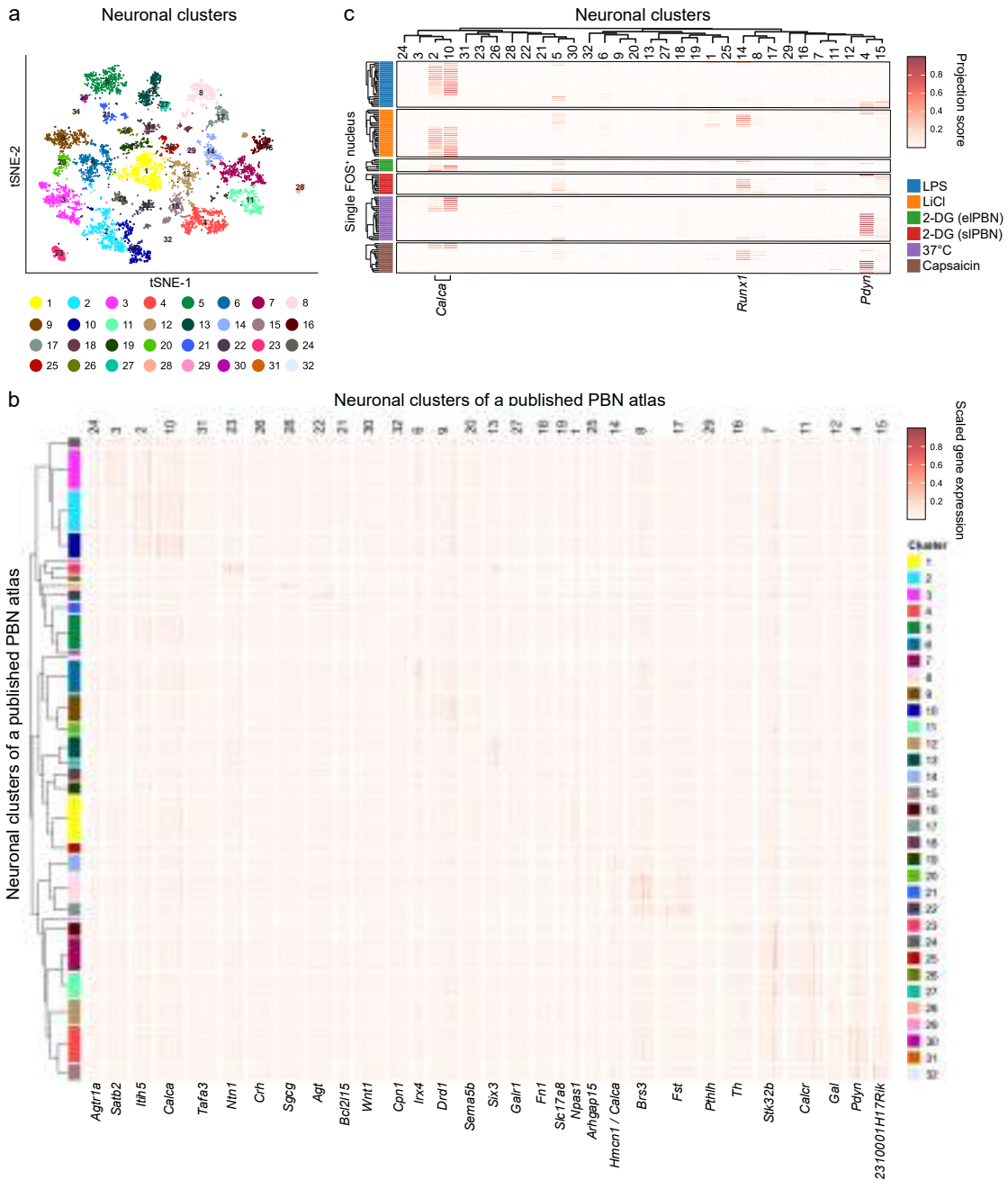

Extended Data Fig. 14 Identification of sparsely activated PBN neurons by LASAR-seq using a published PBN atlas as reference.

a, tSNE plot of PBN neuronal clusters from a published scRNA-seq dataset. **b**, Heatmap of cluster-specific marker genes of PBN neurons (see Supplementary Table 3 for marker gene list). **c**, Label transfer analysis of LASAR-seq identifying activated neuronal types in response to different stimuli (heatmap with key marker genes labeled at the bottom).

Extended Data Fig. 15

Extended Data Fig. 15 Single-nucleus atlas of POA neurons served as reference.

a, tSNE plot of POA neuronal clusters. **b**, Heatmap of cluster-specific marker genes (see Supplementary Table 4 for marker gene list). **c**, Bubble plot showing previously reported major neuronal types in the POA with representative markers and dedicated functions.

Extended Data Fig. 16

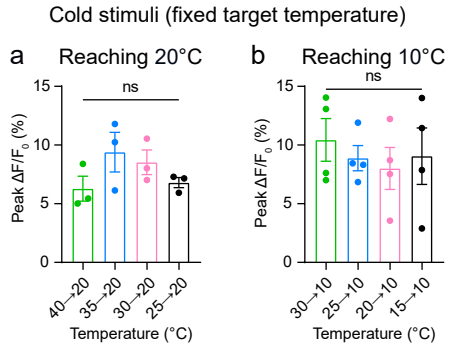

Extended Data Fig. 16 Ca^{2+} responses of *Gpr101*$^{+}$ preoptic neurons to the cold stimuli with different fixed target temperatures.

a-**b**, Bar plot of peak $\Delta F/F_0$ values of Ca^{2+} response in *Gpr101*$^{+}$ preoptic neurons during the cold stimuli with target temperature at 20°C (**a**, n=3 mice per group) or 10°C (**b**, n=4 mice per group). Mean ± SEM is shown in the bar plots. Statistical significance was analyzed using two-tailed Mann-Whitney test in **a** and **b**.

Extended Data Fig. 17

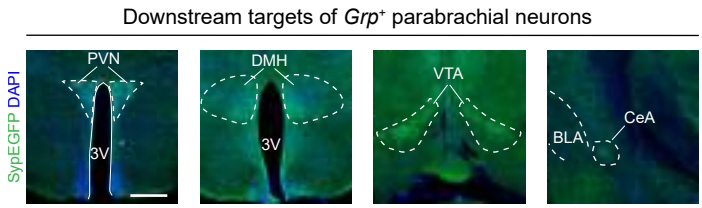

Extended Data Fig. 17 Downstream targets of *Grp*^{PBN} neurons in the brain.

Downstream targets of *Grp*^{PBN} neurons in the brain were studied by examining the AAV-introduced SypEGFP expression in *Grp-Cre* mice (as shown in **Fig. 4a**). EGFP immunostaining revealed presynaptic terminals of the *Grp*^{PBN} neurons in the PVN (paraventricular nucleus), DMH (dorsomedial hypothalamus), VTA (ventral tegmental area), and CeA (central nucleus of the amygdala). Scale bar: 500 μm.

Extended Data Fig. 18

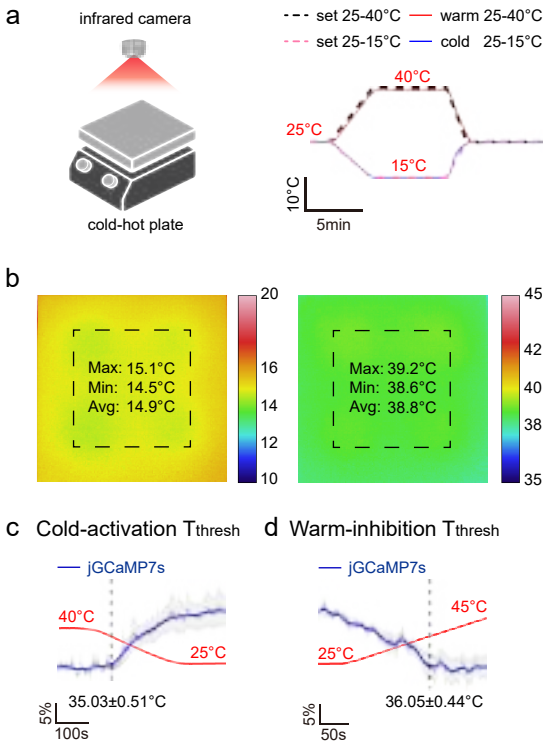

Extended Data Fig. 18 Estimation of temperature thresholds of *Grp*^{PBN} neurons.

a, Scheme of a cold-hot plate, and an infrared camera used to evaluate the spatial temperature distribution in the plate (left panel). Calibration of the cold-hot plate setting vs. actual floor temperatures measured by a BAT-12 Physitemp thermal probe (right panel, n=4). **b**, Infrared thermal imaging showed spatial temperature homogeneity in the cold-hot plate. Mice under anesthesia were positioned centrally (within the area marked by dashed lines), where the spatial temperature was homogeneous. **c**-**d**, Estimation of the temperature thresholds to activate (**c**) or inhibit (**d**) the *Grp*$^{+}$ neurons in the PBN (n=8 mice). The actual averaged floor temperature was measured by a thermal probe (red traces).

Supplementary table legends

Supplementary Table 1. A marker gene list of *Slc17a6*$^{+}$ parabrachial neuronal types classified using the snRNA-seq dataset of the PBN of mice at unstimulated status in this paper.

Supplementary Table 2. A marker gene list of *Slc17a6*$^{+}$ parabrachial neuronal types classified using the snRNA-seq dataset of the PBN in cold-stimulated mice in this paper.

Supplementary Table 3. A marker gene list of *Slc17a6*$^{+}$ parabrachial neuronal types classified using a published snRNA-seq dataset of the PBN. (Pauli, J.L., *et al*. eLife 2022, *11*, e81868.)

Supplementary Table 4. A marker gene list of neuronal types classified using the snRNA-seq dataset of the POA in this paper.